Neutral Surfaces

TREVOR J. MCDOUGALL

CSIRO Division of Oceanography, GPO Box 1538 Hobart, TAS 7001, Australia

(Manuscript received 3 February 1987, in final form 6 May 1987)

ABSTRACT

Scalar properties in the ocean are stirred (and subsequently mixed) rather efficiently by mesoscale eddies and two-dimensional turbulence along "neutral surfaces", defined such that when water parcels are moved small distances in the neutral surface, they experience no buoyant restoring forces. By contrast, work would have to be done on a moving fluid parcel in order to keep it on a potential density surface. The differences between neutral surfaces and potential density surfaces are due to the variation of α/β with pressure (where α is the thermal expansion coefficient and β is the saline contraction coefficient).

By regarding the equation of state of seawater as a function of salinity, potential temperature, and pressure, rather than in terms of salinity, temperature, and pressure, it is possible to quantify the differences between neutral surfaces and potential density surfaces. In particular, the spatial gradients of scalar properties (e.g., S, θ, tritium or potential vorticity) on a neutral surface can be quite different to the corresponding gradients in a potential density surface. For example, at a potential temperature of 4°C and a pressure of 1000 db, the lateral gradient of potential temperature in a potential density surface (referenced to sea level) is too large by between 50% and 350% (depending on the stability ratio R_ρ of the water column) compared with the physically relevant gradient of potential temperature on the neutral surface. Three examples of neutral surfaces are presented, based on the Levitus atlas of the North Atlantic.

1. Introduction

As a fluid parcel moves around the ocean and experiences a variety of pressures, its in situ density continually changes because of the compressibility of seawater. Water parcels do not, then, move on surfaces of constant in situ density. In order to reduce this variation of density, Wust (1933) and Montgomery (1938) defined a new variable, namely potential density, which is the density that a fluid parcel would have if it were moved isentropically and adiabatically to an arbitrarily chosen, but fixed, reference pressure (actually Montgomery used σ_t as an approximation to σ_θ). Ekman (1934), in a published review of the paper by Wust (1933), first pointed out that the vertical gradient of potential density was not an appropriate measure of the vertical stability of the water column.

Neutral surfaces are defined so that small isentropic and adiabatic displacements of a fluid parcel in a neutral surface do not produce a buoyant restoring force on the parcel. In this way, fluid parcels can be exchanged and mixed over small distances in the neutral surface without having to supply gravitational potential energy. Fluxes of properties across neutral surfaces require work to be done against the restoring force of gravity and these fluxes are several orders of magnitude less than the lateral property fluxes. This definition of a neutral surface is the same as that used by Pingree (1972) and Ivers (1975), and it serves to define the local tangent plane of the neutral surface. By defining the surface in terms of the conservative thermodynamic variables, potential temperature and salinity, it proves to be possible to obtain expressions for the differences between the neutral surface and a potential density surface. This is not possible if neutral surfaces are defined in terms of *local* potential densities which have continually changing reference pressures.

Neutral surfaces differ from potential density surfaces because the compressibility of seawater is a function of salinity and potential temperature (or, equivalently, because α/β is dependent on pressure, where α is the thermal expansion coefficient and β is the saline contraction coefficient). The deficiencies of potential density surfaces have been known for some time. For example, Lynn and Reid (1968), Reid and Lynn (1971), Ivers (1975) and Reid (1981) have cleverly reduced the errors associated with using potential density surfaces by using three different reference pressures namely, 0, 2000 and 4000 db. The use of a reference pressure of 4000 db has since become standard practice for studies of deep-ocean circulation. In the present paper, a formalism is developed that readily quantifies the differences between the types of surfaces. For example, given the ranges of pressure and potential temperature on such a surface, one can calculate the variation of potential density on the neutral surface, and on the basis of this, decide if a potential density surface is sufficiently accurate for one's application.

An important result of this paper is that a map of a scalar property on a neutral surface can be surprisingly

different from the corresponding map on a potential density surface. For example, at a depth of 1500 m in the North Atlantic, under the Mediterranean tongue, the spatial gradient of potential temperature in the potential density surface is four times as large as the physically relevant spatial gradient of potential temperature in the neutral surface at the same point.

2. Definition and Properties of a neutral surface

While the International Equation of State of seawater expresses the in situ density ρ as a function of salinity S, in situ temperature T and in situ pressure p, that is,

$$\rho = \hat{\rho}(S, T, p), \tag{1}$$

it is convenient for theoretical studies to define a different functional form for the equation of state, namely,

$$\rho = \rho(S, \theta, p, p_r) \tag{2}$$

where θ is the potential temperature, defined by

$$\theta = \theta[S, T, p, p_r] = T + \int_p^{p_r} \Gamma[S, t = \theta(S, T, p, p'), p']dp', \tag{3}$$

and Γ is the adiabatic lapse rate in units of °C db^{-1}. Apart from the very small effects of the "heat of mixing" (Mamayev, 1975), potential temperature is a conservative intensive thermodynamic variable (see McDougall, 1987, for a discussion of these very small nonlinear thermodynamic terms). In order to motivate the definition of a "neutral surface", the above equations of state, (1) and (2), will first be used to find two equivalent expressions for the buoyancy frequency N, which is defined by

$$\rho g^{-1} N^2 = -\frac{d\rho}{dz} + \left.\frac{d\rho}{dz}\right|_{\substack{\text{isentropic} \\ \text{adiabatic}}}. \tag{4}$$

Here $d\rho/dz$ is the vertical gradient of in situ density, which is measured from, say, a CTD cast; the second term on the right-hand side of (4) represents the change in in situ density that the fluid parcel at (S, T, p) would experience during small vertical excursions if these excursions were performed isentropically and adiabatically. For the normal equation of state, (1), the above definition of N^2, (4), leads to

$$g^{-1} N^2 = \hat{\alpha}(T_z - g\rho\Gamma) - \hat{\beta} S_z \tag{5}$$

where

$$\hat{\alpha} = -\frac{1}{\rho}\left.\frac{\partial \hat{\rho}}{\partial T}\right|_{S,p} \tag{6}$$

$$\hat{\beta} = \frac{1}{\rho}\left.\frac{\partial \hat{\rho}}{\partial S}\right|_{T,p}. \tag{7}$$

The alternative functional form of the Equation of State, (2) leads to

$$g^{-1} N^2 = \alpha\theta_z - \beta S_z \tag{8}$$

where

$$\alpha = -\frac{1}{\rho}\left.\frac{\partial \rho}{\partial \theta}\right|_{S,p} = \hat{\alpha}\left[\left.\frac{\partial \theta}{\partial T}\right|_{S,p}\right]^{-1} \tag{9}$$

$$\beta = \frac{1}{\rho}\left.\frac{\partial \rho}{\partial S}\right|_{\theta,p} = \hat{\beta} + \alpha\left.\frac{\partial \theta}{\partial S}\right|_{T,p}. \tag{10}$$

The pressure to which θ is referenced, p_r, is also kept constant in the derivatives in (9) and (10). For further details on the above equations the reader is referred to McDougall (1984) or Gill (1982) (where Eqs. 8–10 are first derived in the literature).

The buoyancy frequency N is defined in terms of vertical density gradients and when $N^2 = 0$ the water column is said to be "neutrally stable". This means that fluid parcels can be interchanged over small vertical distances without requiring any work to be done against buoyant restoring forces. Consider now a region of the ocean where $N^2 > 0$ and imagine moving a fluid parcel isentropically and adiabatically small distances in a variety of directions. For some directions of movement (close to horizontal), the new in situ density of the parcel will be equal to that of the surroundings and no gravitational potential energy will have been expended. There is, in fact, a plane in which the fluid parcel can be moved small distances without experiencing a buoyant restoring force. Figure 1 is a sketch of two points, a and b, that lie a small distance apart in such a plane of neutral buoyancy. The change of in situ density of a fluid parcel when moved from a to b adiabatically and isentropically (i.e., at constant θ and S) is given by $\rho\gamma[p(\text{b}) - p(\text{a})]$ where γ is the adiabatic and isentropic compressibility defined by

$$\gamma = \frac{1}{\rho}\left.\frac{\partial \rho}{\partial p}\right|_{\theta,S} = \frac{1}{\rho}\left.\frac{\partial \hat{\rho}}{\partial p}\right|_{T,S} + \alpha\left.\frac{\partial \theta}{\partial p}\right|_{S,T}. \tag{11}$$

The neutral surface is then defined so that

$$\lim_{\delta x \to 0} \frac{\rho(\text{b}) - \rho(\text{a})}{\delta x} = \lim_{\delta x \to 0} \rho\gamma \frac{[p(\text{b}) - p(\text{a})]}{\delta x}. \tag{12}$$

A neutral surface gradient operator, ∇_n, can be defined by

$$\nabla_n = \left.\frac{\partial}{\partial x}\right|_n \mathbf{i} + \left.\frac{\partial}{\partial y}\right|_n \mathbf{j}, \tag{13}$$

where x and y are the horizontal coordinates and $\mathbf{i}$ and

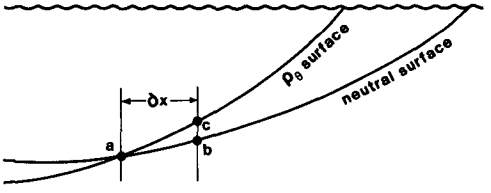

FIG. 1. Sketch of a cross section through the ocean showing a neutral surface and a potential density surface passing through point a. At a horizontal distance δx from point a, a vertical cast cuts the two surfaces at points b and c.

j are the unit vectors in these directions and the neutral surface is defined by

$$\frac{1}{\rho}\nabla_n\rho = \gamma\nabla_n p. \tag{14}$$

Since ρ is a function of S, θ and p, this definition is equivalent to

$$\boxed{\alpha\nabla_n\theta = \beta\nabla_n S.} \tag{15}$$

This form of the definition of the neutral surface proves to be the most useful because it is a relationship between spatial gradients of conservative thermodynamic variables, θ, and S, whereas the alternative definition, (14), involves the nonconservative variable, in situ density ρ.

Returning to Fig. 1, if one performs the thought experiment of moving parcel a to point c on the potential density surface, one finds that it is more dense than the fluid at c. The only depth where this fluid parcel can happily reside in a stable equilibrium on this vertical cast is at point b on the neutral surface. The above stability argument that has lead to the defining equations, (14) or (15), is identical to that used by Pingree (1972) and Ivers (1975) in their work on neutral surfaces.

Defining the neutral surface so that lateral motion and mixing occurs without doing work against gravity does not imply that there is no increase in gravitational potential energy caused by other internal mixing processes in the ocean. Rather, these types of mixing processes (e.g., breaking internal waves, double-diffusive convection, cabbeling, and thermobaricity) are *vertical* in nature and produce dianeutral fluxes that are three or four orders of magnitude less than the lateral property fluxes. In fact, the rate of change of gravitational potential energy caused by these vertical mixing processes is often inferred these days by measuring the rate of dissipation of kinetic energy at the microscale, and applying an assumed flux Richardson number. Because of the vast contrast in the magnitudes of lateral and vertical mixing, it is obviously important to distinguish clearly between them, and in particular, to establish the surfaces along which the strong lateral mixing occurs. The objective of this paper is to develop a quantitative understanding of these surfaces, and to develop simple mathematical expressions that quantify the differences between a neutral surface and a potential density surface in any oceanographic situation. By doing so, there is no implication that vertical mixing and vertical advection processes do not exist in the ocean; rather, these processes are additional to the strong lateral mixing processes that are considered in this paper.

a. *Tangency of locally referenced potential density surfaces and neutral surfaces*

Potential density, ρ_θ is defined by the thought process of moving water parcels adiabatically and isentropically from the in situ pressure p to a reference pressure p_r. (See Fofonoff, 1985, for a very clear discussion of the thermodynamic properties of seawater.) When the water parcel arrives at p_r, its in situ temperature is equal to the potential temperature, $\theta = \theta[S, T, p, p_r]$, and its in situ density is equal to ρ_θ. Both salinity, S, and potential temperature, θ, are conserved during such adiabatic and isentropic displacements, whereas the in situ temperature and in situ density are not. From this discussion, potential density is given by

$$\rho_\theta = \hat{\rho}[S, t = \theta(S, T, p, p_r), p_r] = \rho(S, \theta, p_r) \tag{16}$$

where t is a dummy variable representing in situ temperature at any pressure other than the original pressure p of the water parcel.

In a similar fashion to the definition (13) of lateral gradients of properties on a neutral surface, the lateral gradients of a property on a potential density surface are defined by

$$\left.\frac{\partial\varphi}{\partial x}\right|_\sigma = \lim_{\delta x\to 0}\frac{\varphi(\mathrm{c}) - \varphi(\mathrm{a})}{\delta x} \tag{17}$$

$$\nabla_\sigma\varphi = \left.\frac{\partial\varphi}{\partial x}\right|_\sigma \mathbf{i} + \left.\frac{\partial\varphi}{\partial y}\right|_\sigma \mathbf{j}, \tag{18}$$

where points a and c lie on the same potential density surface (see Fig. 1) and the subscript σ implies that potential density ρ_θ ($=\sigma_\theta + 1000$ kg m^{-3}) is held constant during differentiation.

The lateral gradient of potential density in the potential density surface is, of course, zero, and this can be expressed in terms of the corresponding gradients of S and θ (from 16) by

$$\rho_\theta^{-1}\nabla_\sigma\rho_\theta = 0 = \beta(p_r)\nabla_\sigma S - \alpha(p_r)\nabla_\sigma\theta. \tag{19}$$

Note that the spatial gradients $\nabla_\sigma S$ and $\nabla_\sigma\theta$ are defined at the subsurface point a of Fig. 1 rather than at p_r, and that $\alpha(p_r)$ and $\beta(p_r)$ are simply shorthand ways of writing $\alpha(S, \theta, p_r)$ and $\beta(S, \theta, p_r)$. The relationship between the lateral gradients of S and θ on the potential density surface can now be written in the convenient form

$$\boxed{\alpha(p_r)\nabla_\sigma\theta = \beta(p_r)\nabla_\sigma S.} \tag{20}$$

Note that the corresponding relationship (15) between the lateral gradients of S and θ on the neutral surface involves α and β evaluated at the in situ pressure p, whereas (20) involves $\alpha(p_r)$ and $\beta(p_r)$. Note also that the potential density surface is not a surface on which fluid parcels can be moved without experiencing buoyancy forces. Points lying on the same potential density surface can be freely moved about in this fashion *at the reference pressure, p_r,* (i.e., after having undergone artificial vertical displacements), but a potential density surface does not have this property at the in situ pressure, p.

When the reference pressure, p_r, is equal to the in situ pressure, p, the ratio α/β is the same in the neutral surface definition (15) and in the relationship (20) that applies along potential density surfaces. This implies that at $p = p_r$, the two surfaces are identical, as illustrated by the tangency of these surfaces in Fig. 2. In this way the neutral surface may be regarded as the envelope of a whole series of locally referenced potential density surfaces.

b. Independence of the definition of neutral surfaces to the reference pressure of potential temperature

It is straightforward to show that the definitions (14) or (15) of the neutral surface apply no matter what reference pressure is chosen for the potential temperature, θ. This is because θ is a conservative intensive thermodynamic variable of state, irrespective of its reference pressure. Consider, for example, two different reference pressures for θ, of say, 0 db and 4000 db. The in situ density (2) has two different functional forms as follows:

$$\rho = \rho_0(S, \theta_0, p, 0), \quad \rho = \rho_4(S, \theta_4, p, 4000) \tag{21}$$

where

$$\theta_0 = \theta[S, T, p, 0], \quad \theta_4 = \theta[S, T, p, 4000]. \tag{22}$$

The neutral surface can be defined by either (from 14)

$$\frac{1}{\rho}\nabla_n\rho = \frac{1}{\rho_0}\nabla_n\rho_0 = \frac{1}{\rho}\frac{\partial\rho}{\partial p}\bigg|_{\theta_0,S}\nabla_n p = \gamma\nabla_n p, \tag{23}$$

or

$$\frac{1}{\rho}\nabla_n\rho = \frac{1}{\rho_4}\nabla_n\rho_4 = \frac{1}{\rho}\frac{\partial\rho}{\partial p}\bigg|_{\theta_4,S}\nabla_n p = \gamma\nabla_n p. \tag{24}$$

During the adiabatic and isentropic displacements used to define the compressibility (γ), S, θ_0 and θ_4 are all conserved, hence γ is independent of the reference pressure chosen for θ, and thus the neutral surface definitions (23) and (24) are the same.

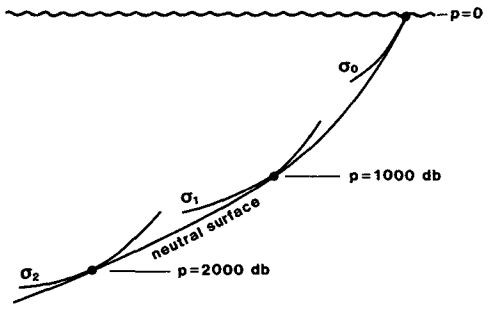

FIG. 2. Sketch of a neutral surface and three different potential density surfaces, referenced to 0 db, 1000 db and 2000 db. The neutral surface is tangential to potential density surfaces only at the reference pressure of those potential density surfaces. In this way, the neutral surface can be regarded as the envelope curve of many locally referenced potential density surfaces with continually changing reference pressures. The definition of a neutral surface adopted in this paper avoids the concept of potential density and in particular, avoids the changing reference pressure which is endemic to a neutral surface defined in terms of potential density concepts.

c. Neutral surfaces and potential density surfaces coincide along potential isotherms

Consider the line of intersection of a neutral surface and a potential density surface. Let s be the curvilinear distance (projected onto the horizontal plane, see McDougall, 1987) along this intersection line. Equations (15) and (20) imply that along this line

$$\alpha\frac{\partial\theta}{\partial s}\bigg|_n = \beta\frac{\partial S}{\partial s}\bigg|_n \tag{25}$$

$$\alpha(p_r)\frac{\partial\theta}{\partial s}\bigg|_\sigma = \beta(p_r)\frac{\partial S}{\partial s}\bigg|_\sigma. \tag{26}$$

Also along this line,

$$\frac{\partial\theta}{\partial s}\bigg|_n = \frac{\partial\theta}{\partial s}\bigg|_\sigma$$

$$\frac{\partial S}{\partial s}\bigg|_n = \frac{\partial S}{\partial s}\bigg|_\sigma. \tag{27}$$

These four equations are satisfied if, and only if, θ and S are constant along the intersection line, implying that potential density surfaces and neutral surfaces intersect along potential isotherms and isohalines. This result also implies that the lateral gradient vectors $\nabla_n\theta$, $\nabla_\sigma\theta$, $\nabla_n S$ and $\nabla_\sigma S$ are all parallel. Note that the lateral gradients of other passive tracers (i.e., other than θ and S) in the two surfaces need not be parallel. Figure 3 shows a vertical cross section of a neutral surface and a potential density surface meeting at two points A and B. The above result implies that points A and B have the same salinity and potential temperature and that at these two points $\nabla_n\theta$ and $\nabla_\sigma\theta$ are parallel. Note that the gradient vectors $\nabla_n\theta$ and $\nabla_\sigma\theta$ in these two different surfaces need not be parallel at points other than the intersection points, A and B.

3. Lateral gradients of scalars on neutral surfaces compared with those on potential density surfaces

Returning to Fig. 1, note that the differences between θ and S on the two surfaces appear also as vertical property differences. Since the angle between the neutral surface and the potential density surface can be defined both in terms of θ as $(\nabla_\sigma\theta - \nabla_n\theta)/\theta_z$ and in terms of S as $(\nabla_\sigma S - \nabla_n S)/S_z$, we have

$$(\nabla_\sigma\theta - \nabla_n\theta) = \frac{\theta_z}{S_z}(\nabla_\sigma S - \nabla_n S). \tag{28}$$

Note that the lateral distances involved in the lateral

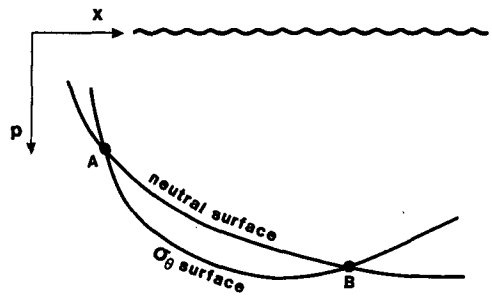

FIG. 3. Cross section of a neutral surface and a potential density surface that intersect at two points A and B. It is shown that these points have the same potential temperature and salinity. Neutral surfaces and potential density surfaces coincide along lines in three-dimensional space that are potential isotherms and isohalines.

gradient operators, ∇_n and ∇_σ, are measured in the horizontal plane, even though the property changes are evaluated on the undulating surface. This practice is common in meteorology where the nonorthogonal coordinate system is labeled "isobaric" (since their surface is one of constant pressure) and is explained in detail by McDougall (1987) and references contained therein.

From (15), (20) and (28), the spatial gradients of potential temperature in the two surfaces are related by

$$\boxed{\nabla_\sigma\theta = \frac{c[R_\rho - 1]}{[R_\rho - c]}\nabla_n\theta} \tag{29}$$

where

$$R_\rho = \frac{\alpha\theta_z}{\beta S_z} \tag{30}$$

$$c = \frac{\alpha(S,\theta,p)/\beta(S,\theta,p)}{\alpha(S,\theta,p_r)/\beta(S,\theta,p_r)}. \tag{31}$$

The corresponding result for the spatial gradients of salinity is

$$\boxed{\nabla_\sigma S = \frac{[R_\rho - 1]}{[R_\rho - c]}\nabla_n S.} \tag{32}$$

In order to use these results, the ratio c of the expansion coefficients is required as a function of pressure. This is plotted in Fig. 4 for $S = 35$ psu and for the reference pressure of the potential density equal to 0 db. The ratio α/β is given by a polynomial in S, θ and p in the Appendix. Note that if c were equal to one, the two surfaces would coincide. It is the variation of α/β with pressure, given by the parameter c, that causes the surfaces to diverge.

As an example, consider a point in the ocean at a pressure of 1000 db, a potential temperature of 4°C and salinity of 35 psu, giving $c \approx 1.25$. If R_ρ is 2, then $\nabla_\sigma\theta$ is 67% larger than $\nabla_n\theta$ (i.e., $c[R_\rho - 1]/[R_\rho - c] = 1.67$) while $\nabla_\sigma S$ is 33% larger than $\nabla_n S$. A more extreme example occurs when R_ρ approaches c. If, for example, $R_\rho = 1.35$ and $c = 1.25$ (as it is under the tongue of Mediterranean Water in the North Atlantic at a depth of 1200 db) then $\nabla_\sigma\theta$ is 4.4 times $\nabla_n\theta$.

Figure 5 shows the ratio of the spatial gradients of potential temperature in the potential density surface to that in the neutral surface, $c[R_\rho - 1]/[R_\rho - c]$, as a function of the vertical stability ratio R_ρ for a fixed value of $c = 1.2$. When the water column is stratified in the "diffusive" sense (cool fresh fluid above warm salty fluid) $c[R_\rho - 1]/[R_\rho - c]$ is less than 1. In general, the ratio $|\nabla_\sigma\theta|/|\nabla_n\theta|$ deviates significantly from 1 when the water column is conducive to either type of double-diffusive convection. When $c = R_\rho$, it can be shown that the vertical gradient of potential density is zero, even though N^2 is not equal to zero.

The corresponding results for a tracer, φ, other than θ and S can be found as follows. It is important to note that $\nabla_\sigma\varphi$, $\nabla_n\varphi$ and $\nabla_n\theta$ need not be parallel. Therefore it is prudent to write the relations in terms of a one-dimensional derivative in any particular horizontal direction. The geometry of Fig. 1 now implies that

$$\left.\frac{\partial\varphi}{\partial r}\right|_\sigma = \left.\frac{\partial\varphi}{\partial r}\right|_n + \frac{\varphi_z}{\theta_z}\left.\frac{\partial\theta}{\partial r}\right|_n \left[\frac{\partial\theta/\partial r|_\sigma}{\partial\theta/\partial r|_n} - 1\right] \tag{33}$$

$$= \left.\frac{\partial\varphi}{\partial r}\right|_n + \frac{\varphi_z}{\theta_z}\left.\frac{\partial\theta}{\partial r}\right|_n \frac{R_\rho[c-1]}{[R_\rho - c]} \tag{34}$$

$$= \left.\frac{\partial\varphi}{\partial r}\right|_n + \frac{\varphi_z}{S_z}\left.\frac{\partial S}{\partial r}\right|_n \frac{[c-1]}{[R_\rho - c]}, \tag{35}$$

where r is the distance in any horizontal direction (e.g., x, y or some direction in between the x and y directions).

4. Maps of scalars on three neutral surfaces in the North Altantic

Three neutral surfaces in the North Atlantic were found from the Levitus (1982) dataset. A particular

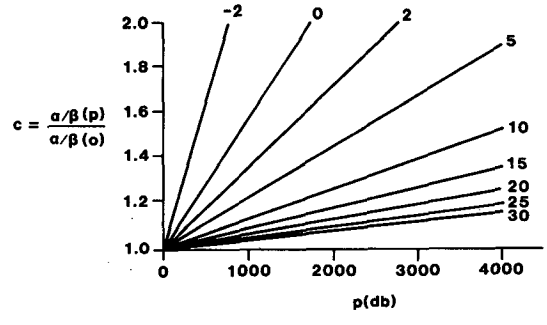

FIG. 4. Plots of the parameter $c = \frac{\alpha}{\beta}(p)\Big/\frac{\alpha}{\beta}(p_r)$ for $S = 35.0$ psu and for various values of θ ($\theta = -2$°C, 0°C, 2°C · · · 30°C) as a function of pressure. The reference pressure, p_r, is 0 db in this figure.

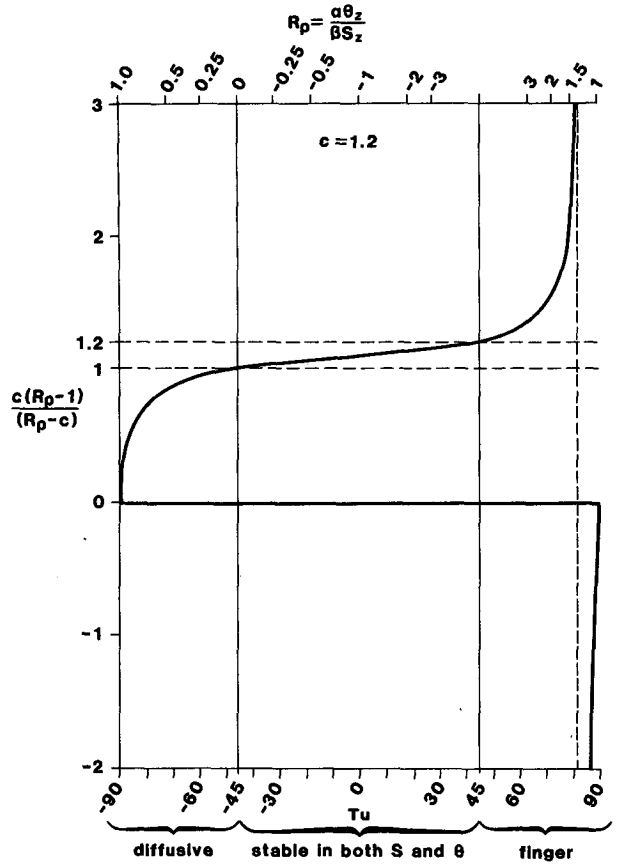

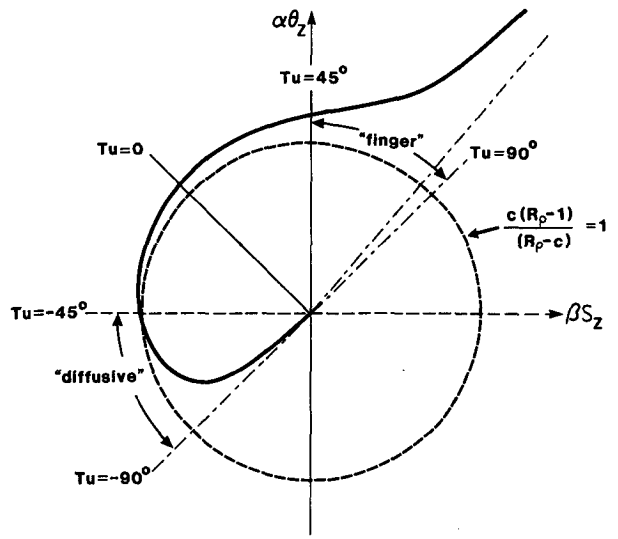

FIG. 5. Graph of the ratio of the lateral gradients of potential temperature in the potential density surface to that in the neutral surface, $c[R_\rho - 1]/[R_\rho - c]$ for an assumed value of $c = 1.2$. In (a) the abscissa is linear in the Turner angle, $\mathrm{Tu} = \arctan(\alpha\theta_z - \beta S_z, \alpha\theta_z + \beta S_z)$, and (b) is a radial plot of the same ratio, $c[R_\rho - 1]/[R_\rho - c]$, as a function of (Tu).

depth at the southwestern corner of the region of interest was selected and then the surface was found by integrating eastward at constant latitude, so that the change in θ and S in the neutral surface from one cast to the next satisfied $\alpha/\beta\delta\theta - \delta S = 0$ [see (15)]. At each vertical cast, the potential temperature and salinity were fitted by a quadratic in pressure over six data points in the vertical, three above the neutral surface and three below. The value of α/β at the previous cast on the neutral surface and the relation $\alpha/\beta\delta\theta - \delta S = 0$ gave a quadratic to solve for the pressure on the neutral surface at the new cast. Strictly speaking, α/β should be evaluated at the midpoint values of θ, S and p between the two casts, but for the Levitus dataset, which has a relatively close station spacing of one degree of latitude and longitude, this refinement was not warranted. Having integrated to the easternmost point of interest, the rest of the plane was reached by northward integrations from the southern baseline. In fact, the lateral integration around an ocean basin on a neutral surface reveals that the neutral surface is mathematically ill-defined. That is to say, after tracing a neutral surface around an ocean basin, one returns to the initial latitude and longitude at a different depth than that of the starting point. This was first pointed out by Reid and Lynn (1971). In a manuscript in preparation, I show that this effect causes neutral trajectories to have a helical path, with a vertical pitch to the helix of only about 10 m after completing a trip around a whole gyre, and so it is not a significant concern for the purpose of mapping properties on neutral surfaces. However, this process may turn out to be an important cause of vertical upwelling velocities across neutral surfaces in the ocean.

The first neutral surface (called NSa here) was selected to have $\sigma_\theta = 27.75$ at the southwestern corner at 5°N, 47°W. Figure 6 maps the pressure, potential temperature, salinity, and potential density on this neutral surface. The pressure varies from 630 db to just less than 1580 db, while θ ranges from 3.5° to 6.2°C. The salinity contours look very similar to the θ contours because variations of S and θ are compensating on the neutral surface (through the ratio α/β). The potential density varies from $\sigma_\theta = 27.73$ to $\sigma_\theta = 27.83$ on this neutral surface.

In order to gain a better feel for the contrast between this neutral surface and potential density surfaces, the pressure on two potential density surfaces are shown in Fig. 7. These potential densities are $\sigma_\theta = 27.73$ and $\sigma_\theta = 27.83$, equal to the minimum and maximum values of potential density that occur on NSa. The $\sigma_\theta = 27.73$ surface coincides with NSa near the northwest corner of the maps, while the $\sigma_\theta = 27.83$ surface and NSa cross each other near the 6°C θ contour [Fig. 6(b)] near the Straits of Gibraltar. Imagine placing a tracer (red dye) in the northwest portion of these maps at a pressure of, say, 700 db on the $\sigma_\theta = 27.73$ surface. On the basis of the potential density map (Fig. 7a), one

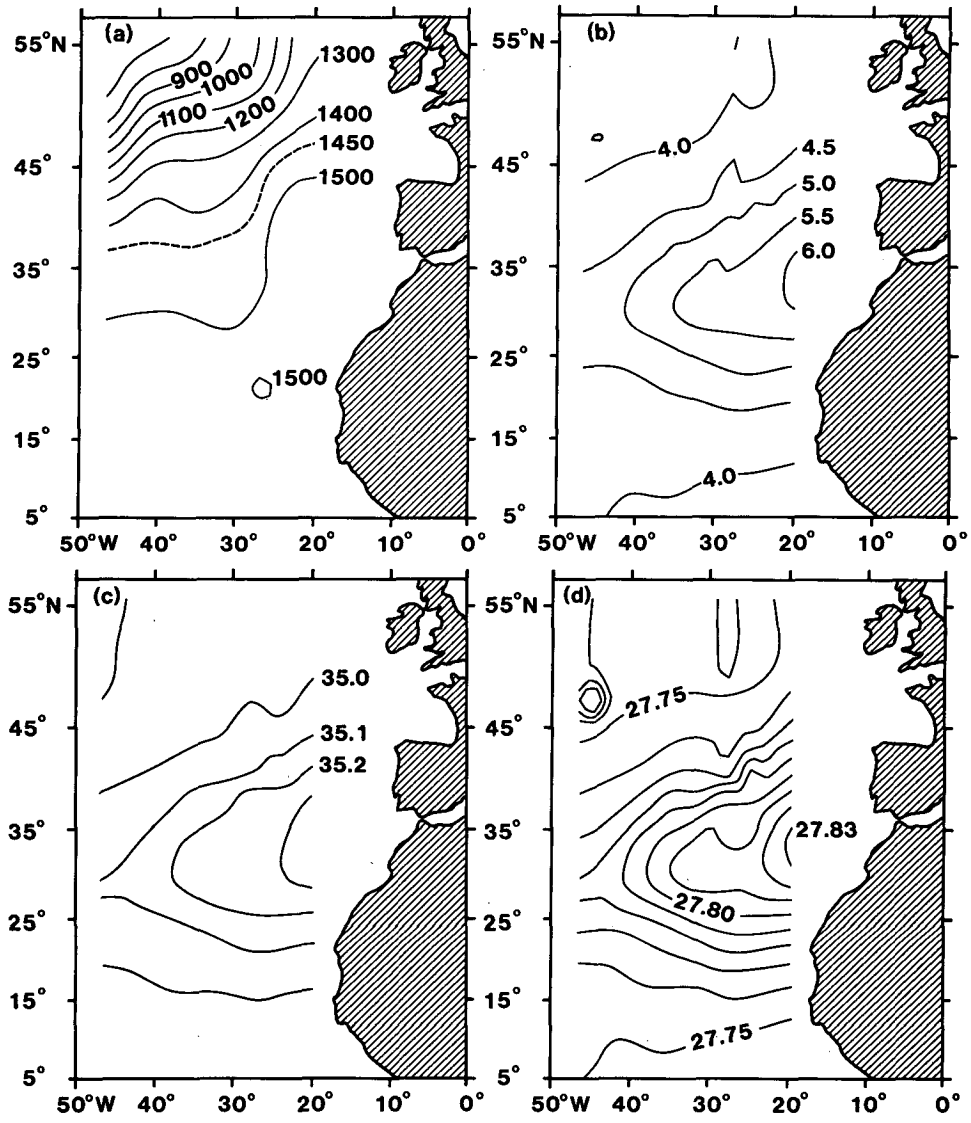

FIG. 6. Maps of (a) pressure, (b) potential temperature, (c) salinity, and (d) σ_θ, in neutral surface NSa, which has $\sigma_\theta = 27.75$ in the southwest corner at 5°N, 47°W.

would expect that when this dye spreads and mixes towards the Straits of Gibraltar, it will be at a pressure of close to 1200 db. However, lateral mixing will cause this dye to mix along the neutral surface rather than along a potential density surface. In addition, vertical mixing processes will act to diffuse the red dye patch in the vertical direction, but at a much slower rate. Cabbeling and thermobaricity will cause an equally slow vertical migration of fluid and dye through the neutral surface. Leaving aside these slow *vertical* mixing and advection processes, Fig. 6(a) shows that the centroid of this dye patch would be deeper than 1500 db by the time it reaches the eastern boundary.

The contrast between the depths of a neutral surface and a potential density surface is even more pronounced between the $\sigma_\theta = 27.83$ surface and NSa. Tracer released at the point of coincidence of these two surfaces (near Spain) would spread along the neutral surface and never be deeper than at the release point (1540 db), while the potential density surface dips down to below 2400 db, where it is at twice the depth of the neutral surface. This is illustrated in the vertical cross section of Fig. 7(c). It is well known that potential density contours are unreliable indicators of the motion and the direction of lateral mixing in the deep North Atlantic, as evidenced for example in the inversion of σ_θ with depth at 4000 m (see Lynn and Reid, 1968; GEOSECS atlas, Bainbridge, 1976). However, the extent to which potential density is unreliable, even at a depth of 1500 m, is surprising. The North Altantic is an extreme example of the differences between the surfaces, not so much because of the strong lateral gradient

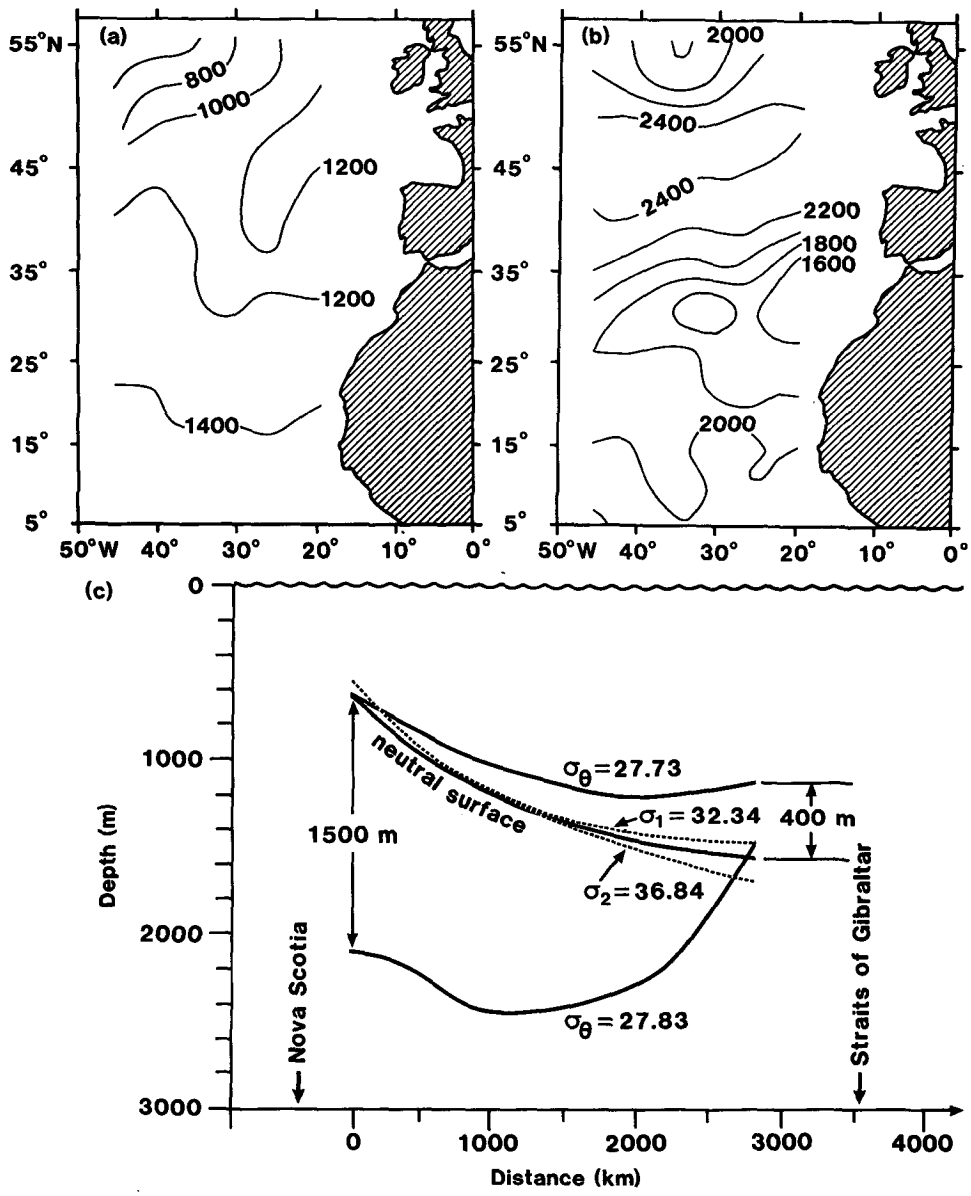

FIG. 7. Maps of pressure on two potential density surfaces: (a) $\sigma_\theta = 27.73$; (b) $\sigma_\theta = 27.83$. The potential density surfaces intersect the same neutral surface (NSa of Fig. 6) at different positions. This is illustrated in cross section in (c), which goes from near Nova Scotia on the left to near the Straits of Gibraltar on the right. Also shown (dashed lines) are a potential density surface referenced to a pressure of 1000 db ($\sigma_1 = 32.34$) and a potential density surface referenced to 2000 db ($\sigma_2 = 36.84$).

of potential temperature due to the Mediterranean Water intrusion, but mainly because R_ρ is quite low [approaching c; see Eqs. (29) and (42)] under the Mediterranean tongue.

Layered models of the ocean circulation use the interface slopes in the thermal wind equation to predict the vertical shear of horizontal velocities, but the marked contrast in the slopes of the surfaces at their points of intersection (shown in Fig. 7c), cautions against using potential density surfaces as dynamically significant interfaces in such models. Because there is mixing in the ocean (lateral and vertical), as evidenced by the variations of θ on neutral surfaces, potential density does not have dynamical significance even if it were a conservative variable (which it is not, due to cabbeling). The main concern of this paper is not, however, the implications of neutral surfaces for dynamical studies of ocean circulation, but the maps of passive tracers on neutral surfaces.

Of course potential densities will still be useful for many types of studies in the ocean, but one must be aware that the very thought process of moving a water

parcel to a reference pressure before assigning a density value to it robs potential density of any strict interpretation in terms of dynamical stability or mixing. The errors involved with using potential density surfaces tend to increase with the difference between the in situ pressure and the reference pressure. By choosing a reference pressure close to the pressure of a dataset, these errors can be minimized. This will subsequently be discussed in more detail, but it is found that a potential density surface referred to 1000 db (σ_1 = 32.34) that intersects the NSa surface at a depth of 1100 db (i.e. approximately at the center of NSa) lies 110 db above the neutral surface at the eastern side of Fig. 7(c), while a potential density surface referred to 2000 db (σ_2 = 36.84), which also intersects NSa at a depth of 1100 db, lies 115 m below NSa at the eastern side of Fig. 7(c). It is clear that, at least for this region of the ocean, a vertical excursion of just 440 m is sufficient to cause a vertical separation between a neutral surface and the *best* (locally referenced) potential density surface of greater than 100 m.

The ratio of the lateral gradient of potential temperature in a potential density surface to that in the intersecting neutral surface, $|\nabla_\sigma\theta|/|\nabla_n\theta|$, given by $c[R_\rho - 1]/[R_\rho - c]$, is contoured on NSa in Fig. 8. This shows that the lateral gradient of θ would be overestimated by as much as 350% by plotting θ on a potential density surface at a depth of 1500 m. Figure 9 shows four maps of potential temperature on four different surfaces, including θ on NSa for the benefit of comparison. The total range of potential temperature on the neutral surface is 2°C, whereas that on the σ_θ = 27.73 surface is 4.5°C. The σ_θ = 27.83 surface (Fig. 9c) coincides with the neutral surface NSa (Fig. 9a) on the 6°C contour in both figures. Thereafter the maps differ markedly in pattern as well as in magnitude. The potential density surfaces with reference pressures of 1000 and 2000 db have θ ranging from 4° to 6.5°C (σ_1 = 32.34 surface, not shown) and from 4° to 5.5°C (σ_2 = 36.84 surface, Fig. 9d), which is closer, but not equal, to the 4°–6°C range on the neutral surface NSa.

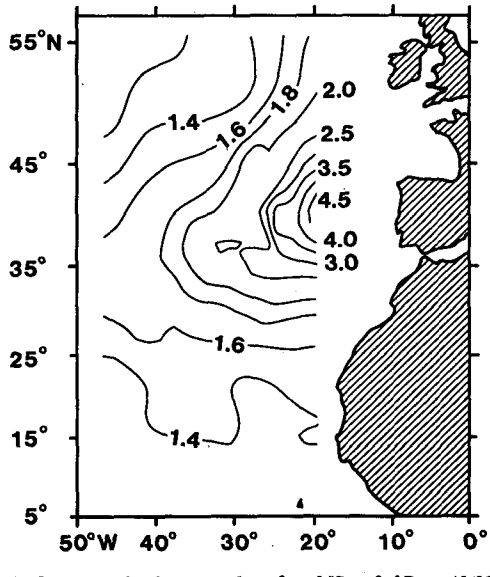

FIG. 8. Contour plot in neutral surface NSa of $c[R_\rho - 1]/[R_\rho - c]$, the ratio of the lateral gradient of θ in a potential density surface, $\nabla_\sigma\theta$, to that in the neutral surface, $\nabla_n\theta$.

The corresponding properties of a shallower neutral surface, NSb, are summarized in Fig. 10. NSb was chosen to have a potential density of 27.30 at the southwest corner. The maximum value of potential density on this surface is greater than 27.38 kg m^{-3} (Fig. 10c), a range of 0.08 kg m^{-3}, which is similar to the range of 0.1 kg m^{-3} on the deeper neutral surface NSa. The ratio $|\nabla_\sigma\theta|/|\nabla_n\theta|$, shown in Fig. 10(d), varies from 1.1 to 1.2. The potential density surface σ_θ = 27.30 coincides with NSb at the southwest corner and is about 70 m shallower from 25° to 35°N. The potential temperature on the σ_θ = 27.30 surface rises to slightly over 10.8°C (compared with 10.0°C on the neutral surface).

A series of maps on a third neutral surface, NSc, are shown in Fig. 11. This surface was chosen to have σ_θ = 26.80 at the southwest corner, which is now at 12°N, 67°W. The potential density σ_θ varies by only 0.03 on this surface and the maximum difference between $\nabla_\sigma\theta$ and $\nabla_n\theta$ is only 10%.

Takahashi et al. (1985) have estimated the Redfield ratios from analyzing nutrient and potential temperature data on potential density surfaces in several oceans. The method of Takahashi et al. (1985) depends on there being only two source waters on the potential density surface and also requires that the effects of vertical mixing are small. The present paper shows that *lateral* mixing in the ocean occurs along neutral surfaces, rather than along potential density surfaces. Therefore, the property–property regressions that are used in Takahashi et al. (1985) should be performed on data that lie in a neutral surface rather than in a potential density surface. This task has not been attempted here, but the property gradients in the neutral surface have been estimated by extending the methods of section 3 of this paper in order to find the expected changes in the Redfield ratios.

The first stage of the process of determining the Redfield ratios now involves finding the ratio of the lateral gradients of O_2 and θ in the neutral surface,

$$\left.\frac{\partial O_2}{\partial x}\right|_n \Big/ \left.\frac{\partial\theta}{\partial x}\right|_n.$$

This can be related to the corresponding ratio of gradients in the potential density surface

$$\left.\frac{\partial O_2}{\partial x}\right|_\sigma \Big/ \left.\frac{\partial\theta}{\partial x}\right|_\sigma$$

(from the dataset of Takahashi et al.), by using the following equation, which is derived from (29) and (34):

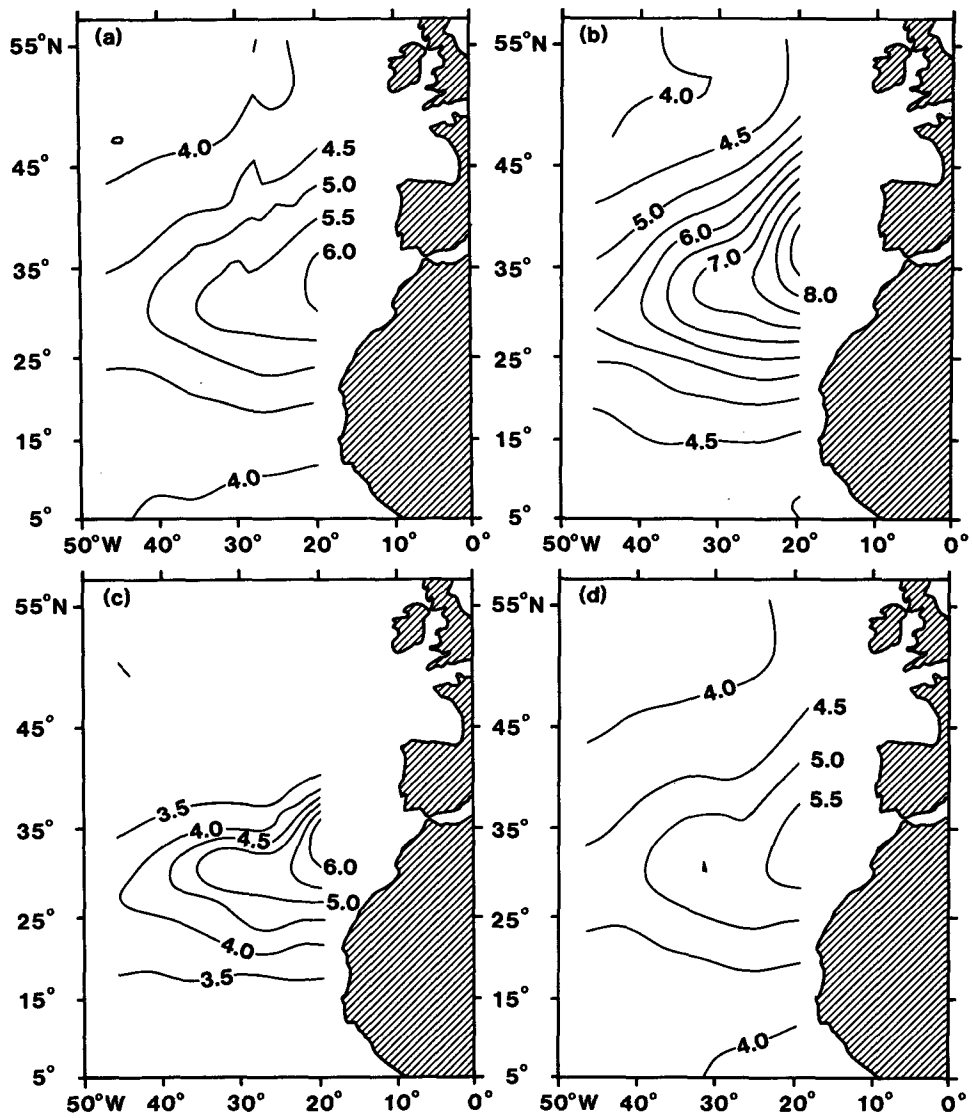

FIG. 9. Potential temperature, θ, mapped (a) on the neutral surface NSa; (b) on the surface $\sigma_\theta = 27.73$; (c) on the surface $\sigma_\theta = 27.83$; and (d) on the surface $\sigma_2 = 36.84$.

$$\left[\left(\frac{\partial O_2}{\partial x}\bigg|_n \Big/ \frac{\partial \theta}{\partial x}\bigg|_n\right) - \left(\frac{\partial O_2}{\partial x}\bigg|_\sigma \Big/ \frac{\partial \theta}{\partial x}\bigg|_\sigma\right)\right] = \left[\left(\frac{\partial O_2}{\partial x}\bigg|_\sigma \Big/ \frac{\partial \theta}{\partial x}\bigg|_\sigma\right) - (O_{2_z}/\theta_z)\right]\frac{R_\rho[c-1]}{[R_\rho - c]}. \quad (36)$$

Having found the new saturation end members of O_2 and θ, the regressions of various properties (PO_4, NO_3, CO_2 and TALK) need to be found as a function of O_2, this data being in the neutral surface rather than in the potential density surface. These regressions can be found from the following equation (φ is any of the four variables) which is also derived along similar lines to the simpler expressions in section 3:

$$\frac{\dfrac{\partial \varphi}{\partial x}\Big|_n - \dfrac{\partial \varphi}{\partial x}\Big|_\sigma}{\dfrac{\partial O_2}{\partial x}\Big|_n - \dfrac{\partial O_2}{\partial x}\Big|_\sigma} = \frac{\dfrac{\partial \varphi}{\partial x}\Big|_\sigma}{\dfrac{\partial O_2}{\partial x}\Big|_\sigma} - \frac{\varphi_z}{O_{2_z}} \times \frac{\left(1-\dfrac{1}{c}\right)}{\left[\dfrac{\theta_z}{O_{2_z}}\left(\dfrac{\partial O_2}{\partial x}\Big|_\sigma \Big/ \dfrac{\partial \theta}{\partial x}\Big|_\sigma\right)\left(1-\dfrac{1}{R_\rho}\right)+1\right]}. \quad (37)$$

These expressions allow us to estimate the spatial variations of properties in the neutral surface in terms of

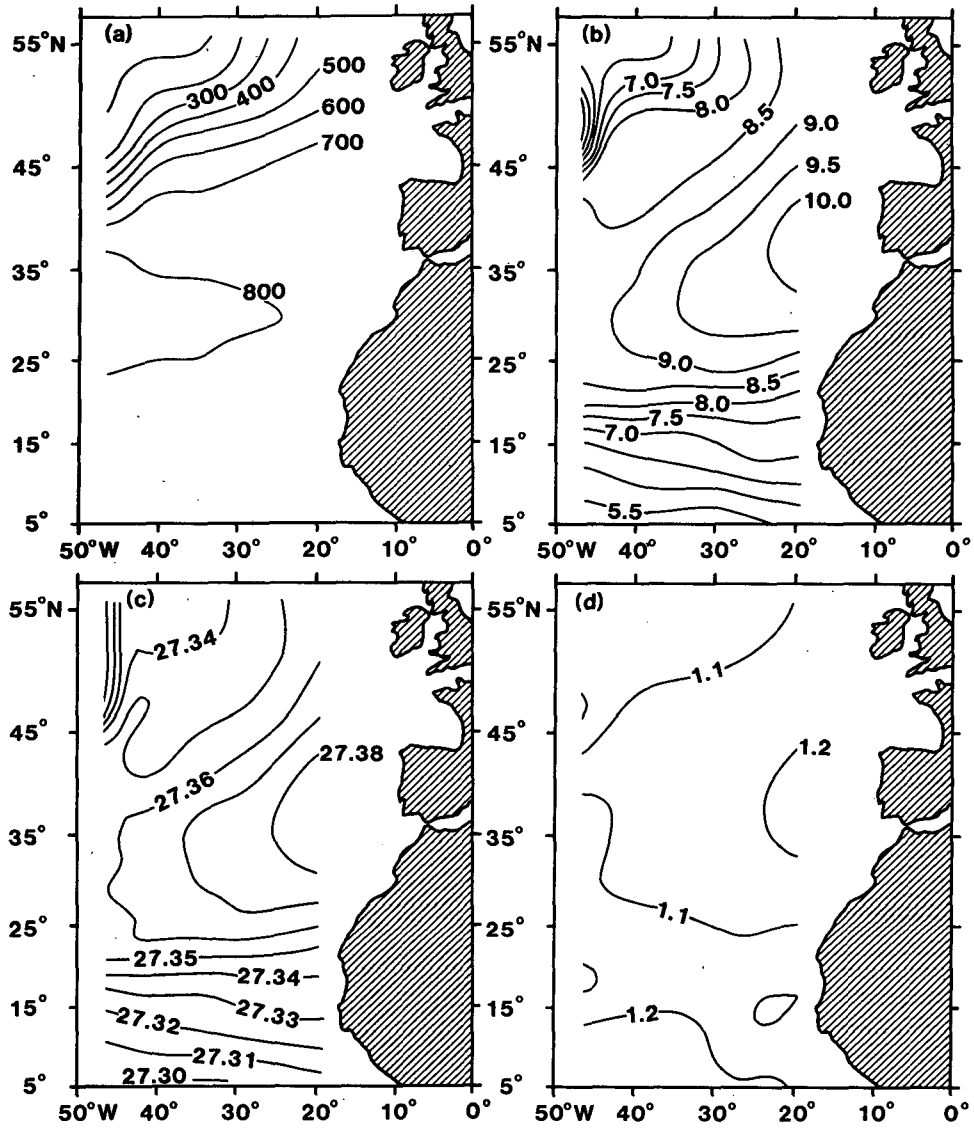

FIG. 10. Maps of (a) pressure, (b) potential temperature, (c) potential density, and (d) the ratio of $|\nabla_\sigma \theta|$ to $|\nabla_n \theta|$, $c[R_\rho - 1]/[R_\rho - c]$, on neutral surface NSb which has $\sigma_\theta = 27.30$ at the southwest corner.

those in the potential density surface and also in terms of the vertical gradients of properties. This information is available in the paper of Takahashi et al. (1985), and has been used here to recalculate the Redfield ratio between the consumption of oxygen and the production of PO_4. The values for the north and south Atlantic oceans on the shallower surface do not change from their values reported by Takahashi et al. (1985), and both are, in fact, 165. However, the deeper surface (originally the $\sigma_\theta = 27.20$ surface, but now a neutral surface) has a ratio of 163 in the North Atlantic (rather than their value of 173) and a ratio of 190 in the South Atlantic (rather than their value of 183). The Redfield ratio for phosphorus, determined by this analysis on a neutral surface, shows more scatter between the different oceans and the different levels than did Takahashi et al.'s own analysis of the same data on potential density surfaces. This scatter could be due to vertical mixing processes (e.g. small-scale turbulence or double-diffusive convection) or to vertical advection processes (cabbeling or thermobaricity), but it may also represent real differences between the biological processes in the different oceans.

5. Quantifying the vertical displacement between a potential density surface and a neutral surface

The discussion so far has concentrated on differences between the lateral gradients of scalar properties in the two types of surfaces. In this section simple expressions

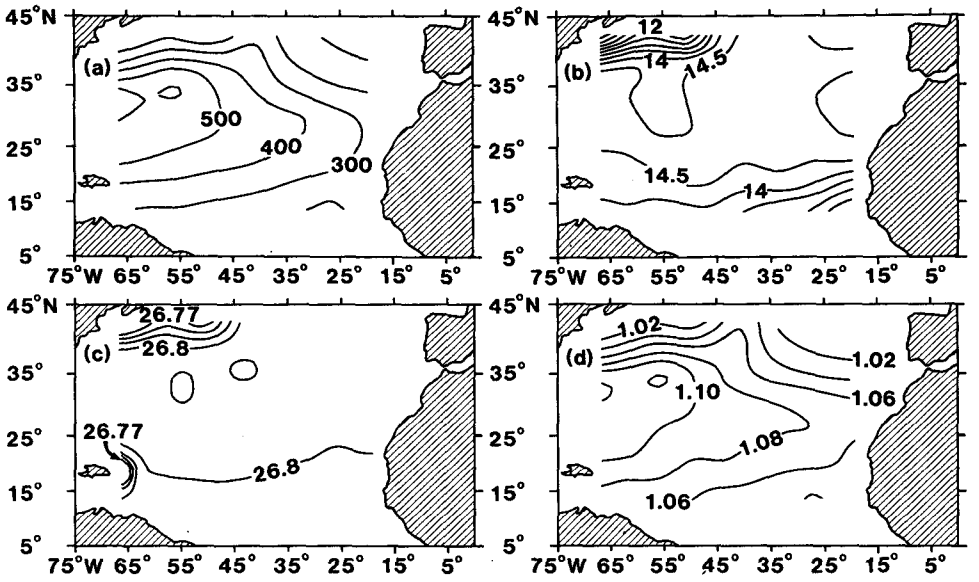

FIG. 11. Maps of properties on a neutral surface, NSc, chosen so that $\sigma_\theta = 26.80$ at the southwest corner of the maps. The maps display (a) pressure, (b) potential temperature θ, (c) potential density σ_θ, and (d) the ratio $|\nabla_c\theta|/|\nabla_n\theta| = c[R_\rho - 1]/[R_\rho - c]$.

are developed for the vertical distance between the surfaces for the purpose of allowing oceanographers to estimate this vertical excursion based on maps of properties in potential density surfaces. In this way, one can determine the magnitude of the errors involved with using a simple potential density surface before one invests the extra effort required to map a neutral surface.

Following the discussion in section 2a, variations of potential density can be related to variations of θ and S by

$$d\rho_\theta = \rho_\theta[\beta(p_r)dS - \alpha(p_r)d\theta] \tag{38}$$

for a fixed reference pressure, p_r. Note that the α and β in (38) are defined by (9) and (10) [rather than by (6) and (7)], and they are evaluated at the reference pressure, p_r, rather than at the in situ pressure p. Along a neutral surface, variations of θ and S are related by $\alpha(p)d\theta = \beta(p)dS$, so that the difference in potential density between two points, a and b, in a neutral surface is given by

$$\rho_\theta{}^b - \rho_\theta{}^a = \int_a^b \rho_\theta\alpha(p_r)[c-1]d\theta$$

$$= \int_a^b \rho_\theta\beta(S,\theta,p_r)\left[\frac{\alpha}{\beta}(S,\theta,p) - \frac{\alpha}{\beta}(S,\theta,p_r)\right]d\theta, \tag{39}$$

where the integral is taken along a neutral surface.

In the Appendix a polynomial expression is given for α/β in terms of the potential temperature, θ, referred to the sea surface (i.e., $p_r = 0$). It can be seen from this polynomial that the differences in α/β at pressure p and at $p_r = 0$ is, to a good approximation, simply equal to $3.4 \times 10^{-5}(p - p_r)$ (psu) $(°C)^{-1}$. This approximation will also apply for potential temperatures (and hence potential densities) referenced to other reference pressures. Also β varies by less than 3% from a value of 0.765×10^{-3} $(\text{psu})^{-1}$ in the oceanographic range of S, θ and p. Taking a value of 1030 kg m^{-3} for ρ_θ in (39) we obtain

$$\rho_\theta{}^b - \rho_\theta{}^a \approx 2.7 \times 10^{-5} \int_a^b (p - p_r)d\theta \text{ kg m}^{-3}, \tag{40}$$

where $(p - p_r)$ is in units of db, and θ is measured in degrees Celsius. This is a very handy approximation because it enables estimates of potential density differences to be made simply from the hydrographic variables p and θ on a neutral surface. As an example of the use of (40), let us calculate the change in ρ_θ (referenced to $p_r = 0$ db) from the 4°C contour to the 6°C contour on neutral surface NSa in Fig. 6(b). Taking $(p - p_r) \approx 1500$ db, (40) gives a potential density difference between these two potential temperature contours of 0.081 kg m^{-3}, in close agreement with Fig. 6(d).

The vertical gradient of potential density, $d\rho_\theta/dz$, $\{=\rho_\theta[\beta(p_r)S_z - \alpha(p_r)\theta_z]\}$ can be expressed in terms of the buoyancy frequency, N, by

$$g^{-1}N^2 = \left[-\frac{1}{\rho_\theta}\frac{d\rho_\theta}{dz}\right]\frac{c[R_\rho - 1]}{[R_\rho - c]}, \tag{41}$$

where the variation of β with pressure has been neglected in comparison with the variation of α with pressure. The depth between a potential density surface and a neutral surface is then given by

$$-\Delta z \approx \frac{c[R_\rho - 1]}{[R_\rho - c]} \frac{g}{N^2} \frac{1}{\rho_\theta} (\rho_\theta{}^b - \rho_\theta{}^a)$$

$$\approx \frac{c[R_\rho - 1]}{[R_\rho - c]} \frac{g}{N^2} \frac{2.7 \times 10^{-5}}{\rho_\theta} \int_a^b (p - p_r) d\theta \quad \text{[m]}. \tag{42}$$

This equation can be used to decide whether the use of a potential density surface will be satisfactory. For example, let us decide that the use of a potential density surface will be satisfactory if it always lies within ±20 m of the neutral surface; if the surfaces diverge by more than this (arbitrarily chosen) 20 m limit, then we must construct the neutral surface or at least resort to using several potential density surfaces referenced to several different intermediate reference pressures. Taking $(-\Delta z) = 20$ m, $c[R_\rho - 1]/[R_\rho - c] = 1.5$, $g = 9.8$ m s^{-2}, $N^2 = 3 \times 10^{-6}$ s^{-2} and $\rho_\theta = 1030$ kg m^{-3}, it is found from (42) that

$$\int_a^b (p - p_r) d\theta \leqslant 150 \text{ db } °\text{C} \tag{43}$$

if $-\Delta z \leqslant 20$ m. If the mean pressure in the region of interest were 1000 db and one were considering using potential density referenced to the sea surface, then (43) shows that a variation of just 0.15°C in θ (or 0.022 psu in S) will cause the potential density surface to diverge from the neutral surface by 20 m in the vertical. However, the usefulness of potential density surfaces can be greatly extended by using a reference pressure at the midpressure of a dataset of interest. For example, imagine that θ and p varied linearly along a neutral surface and that the total change in θ in the region of interest was 3°C. If Δp is the total change in pressure in this same region, the use of a reference pressure, p_r at the average pressure makes the left-hand side of (43) approximately equal to $\Delta p \times 3°\text{C}/8$ and the 20 m excursion limit between the neutral surface and the centrally referenced potential density surface translates into a maximum pressure excursion, Δp of 400 db. Note that if the reference pressure were instead taken to be the maximum or minimum pressure (rather than the average of these), the left-hand side of (43) would be approximately $\Delta p \times 3°\text{C}/2$, and the maximum allowable pressure excursion in the region of interest would be only 100 db. In this way, the sensitivity of potential density surfaces to their reference pressures is apparent. A change of reference pressure of just 200 db can quite easily cause a vertical departure between the surfaces of 80 m, which would be unacceptable for most oceanographic purposes. Armi and Stommel (1983) used great care to reference their potential density surfaces to a series of different reference pressures, each being the mean pressure on that surface in the region of interest. Since they considered a relatively small portion of the ocean, and the excursion of pressure on each surface in their "β triangle" region was less than 400 db, we conclude (using 42) that their surfaces were never more than 20 m from the relevant neutral surface.

The preceding discussion, and equations (40) and (42), are couched in terms of the variations of properties on neutral surfaces. It is also possible to quantify the differences between neutral surfaces and potential density surfaces by using the relationship (29) between $\nabla_n \theta$ and $\nabla_\sigma \theta$ so that the differential of potential temperature that appears in (40) and (42) is weighted by $\{c[R_\rho - 1]/[R_\rho - c]\}^{-1}$ at each point and these integrals can then be evaluated approximately in a potential density surface. This suggests the tractable procedure of first forming a potential density surface and plotting p–θ diagrams in order to evaluate (40) and (42). A neutral surface analysis need only then be performed if some acceptability criterion (like the 20 m excursion limit above) is exceeded.

5. Discussion and conclusions

Scalar properties are transported rather efficiently in the lateral direction in the ocean by the large-scale general circulation and by energetic mesoscale turbulent eddies and two-dimensional turbulent motions. This efficient lateral stirring and mixing occurs along "neutral surfaces" along which no work is required to move fluid parcels small distances. The dianeutral *fluxes* of properties (caused by breaking internal waves, double-diffusive convection, cabbeling and thermobaricity), are typically several orders of magnitude less than the lateral fluxes, but nonetheless they are thought to be responsible for as much subsurface *water mass conversion* because the length scales that transpose fluxes into flux divergences are also different by several orders of magnitude for the two types of processes. The relative importance of lateral and vertical mixing processes for water-mass conversion is then still very much an open question. In an effort to resolve these issues, an increasing number of oceanographic studies use some kind of density horizon in which to plot various scalar properties. The hope is that different tracers will have significantly different vertical and lateral distributions, so that it will be possible to determine the relative importance of lateral and vertical mixing processes by using the data of several tracers simultaneously in an inverse or least-squares procedure. It is traditional to assume that tracers are stirred and mixed along potential density surfaces, although several authors have appreciated the deficiencies of potential density. Since the equation of state of seawater is nonlinear, the surfaces along which scalars are mixed laterally (called "neutral surfaces") can differ significantly from a potential density surface that is referenced to any fixed pressure.

Examples of three neutral surfaces from the North Atlantic have been described in section 4. The lateral gradient of θ on a potential density surface can be more

than four times than on the neutral surface at a depth of only 1500 m. Perhaps even more striking are the vertical separations that can occur between a neutral surface and a potential density surface, as illustrated in Fig. 7. Purposely released tracer material will be mixed along neutral surfaces in the ocean and so may be several hundred meters shallower or deeper than the potential density surface on which the tracer was placed. Even if one were to reference potential density to the pressure of the release point, the example of Fig. 7(c) shows that this density surface could later be more than 100 m deeper or shallower than the neutral surface. These examples from the North Atlantic are rather extreme, due mainly to the fact that R_ρ becomes quite small under the Mediterranean Water tongue, so that $[R_\rho - c]$ becomes small [see (29) and (42)], and also because there are substantial compensating lateral gradients of θ and S in this region of the ocean.

Another example of the difference between neutral surfaces and potential density surfaces occurs when considering the strength of the 15°N front in the Atlantic and Pacific oceans. According to Broecker and Peng, (1982, their Fig. 8.6), this thermocline frontal region has a strength of 3.8°C in the Atlantic and 3.7°C in the Pacific on the $\sigma_\theta = 26.75$ kg m^{-3} horizon. However, the physically relevant contrasts of θ and S must be measured on a neutral surface. Using $c = 1.06$ and $R_\rho = 2$ we find that the θ contrasts across the 15°N fronts in the Atlantic and Pacific are only 3.4° and 3.3°C, respectively.

Jenkins (1987) has plotted (among other things) the tritium–helium age of recently subducted water on a series of potential density surfaces in the β-triangle area of the eastern North Atlantic. Tritium–helium age tends to have large vertical gradients in comparison with its lateral gradients and this can cause substantial differences between maps of tritium–helium age on neutral surfaces compared with those on potential density surfaces. For example, by using Eq. (35) it is found that on the $\sigma_\theta = 27.45$ surface the lateral gradient of age is overestimated by 60% and on the $\sigma_\theta = 27.75$ surface, the lateral gradient of the tritium-helium age is less than one half of that shown by Jenkins (1987).

Having defined neutral surfaces in terms of changes of two conservative, intensive, state variables (S and θ), it is possible to quantify the differences between a neutral surface and a potential density surface. In particular, it is important to be able to distinguish oceanographic situations where the use of a potential density surface of some kind is sufficiently accurate from situations where one must either use a neutral surface or at least use several different potential density surfaces with more closely spaced reference pressures. These decisions can now be based on Eq. (40) which gives a way to quantify the variation of potential density on a neutral surface in terms of the area on a pressure–potential temperature diagram, and on Eq. (42) which quantifies the vertical separation between a neutral surface and a potential density surface.

Acknowledgments. This research was performed during a sabbatical visit to the Woods Hole Oceanographic Institution in 1985. The Center for Analysis of Marine Systems at WHOI is thanked for its hospitality and its generosity in providing partial financial support. The task of producing contour plots was greatly facilitated by the CAMS-ATLAS plotting package (Sgouros and Keffer, 1983). Nikki Pullen did an excellent job with the wordprocessing of this manuscript and Josephine Nunn and Graham Wells prepared the figures for publication. I thank Professor J. L. Reid for some of the early references on the dynamical implications of the equation of state of seawater. This work relies heavily on regarding the in situ density of seawater to be a function of (θ, S, p) rather than of (T, S, p). Dr. Adrian Gill pioneered the use of this form of the equation of state to obtain a simple, but exact, equation for the buoyancy frequency, N, [our Eq. (8)], based on his new thermal expansion and saline contraction coefficients [our Eqs. (9) and (10)]. This paper is dedicated to his memory.

APPENDIX

Polynomial Expressions for α/β and β

The following polynomials have been fitted over the oceanographic ranges of θ, S and p. S was varied from 25 to 40 psu, while p was varied from 0 to 10 000 db (for $\theta = 0$°C), from 0 to 4000 db (for $\theta = 10$°C) and from 0 to 1000 db (for $\theta = 20°$, 30° and 40°C). In this way 248 data points were fitted. The values of α and β are defined in Eqs. (9) and (10) in the text. The partial derivatives of the international equation of state, $\hat{\alpha}$ and $\hat{\beta}$ (defined in terms of S, T and p) were found by mathematically differentiating the international equation of state, using a FORTRAN program written by R. C. Millard of the Woods Hole Oceanographic Institution. This same program was used to generate the tables in Fofonoff and Millard (1984). The partial derivatives of θ with respect to T and S, $\partial\theta/\partial T|_{S,p}$ and $\partial\theta/\partial S|_{T,p}$ were found by mathematically differentiating the polynomial expression for $\theta(S, T, p)$ given by Bryden (1973). The adiabatic and isentropic compressibility of seawater, γ [see Eq. (11)] was found in a similar fashion and the derivations of α, β and γ were finally checked by confirming that $-\partial\alpha/\partial p = \partial\gamma/\partial\theta$, $-\partial\alpha/\partial S = \partial\beta/\partial\theta$, and $\partial\beta/\partial p = \partial\gamma/\partial S$, by taking small increments of $p = 20$ db, $\theta = 0.1$°C and $S = 0.1$ psu.

The following polynomial was fitted to the ratio α/β over the oceanographic range of S, θ and p:

$$\alpha/\beta = +0.665157\times10^{-1} + 0.170907\times10^{-1}\theta - 0.203814\times10^{-3}\theta^2 + 0.298357\times10^{-5}\theta^3$$

$$
\begin{aligned}
&-0.255019\times10^{-7}\theta^4+(S-35.0)\\
&\times\{+0.378110\times10^{-2}-0.846960\times10^{-4}\theta\\
&-0.164759\times10^{-6}p-0.251520\times10^{-11}p^2\}\\
&+(S-35.0)^2\{-0.678662\times10^{-5}\}\\
&+p\{0.380374\times10^{-4}-0.933746\times10^{-6}\theta\\
&+0.791325\times10^{-8}\theta^2\}+0.512857\times10^{-12}p^2\theta^2\\
&-0.302285\times10^{-13}p^3.
\end{aligned}
$$

The rms error of this fit is 0.000894 psu $(°C)^{-1}$ and a check value is 0.34763 psu $(°C)^{-1}$ at S = 40.0 psu, θ = 10.0°C and p = 4000 db. This rms error will not cause significant errors in defining a neutral surface. For example, if θ varies by 3°C on a neutral surface, then a consistent error in α/β over the surface of 0.001 psu $(°C)^{-1}$ will lead to an error of 0.020°C over the neutral surface, equivalent to an error in potential density of only 0.003 kg m^{-3}.

The following polynomial for β was fitted over the sme 248 S, θ, and p values spanning the oceanographic range.

$$
\begin{aligned}
\beta = &+0.785567\times10^{-3}-0.301985\times10^{-5}\theta\\
&+0.555579\times10^{-7}\theta^2-0.415613\times10^{-9}\theta^3\\
&+(S-35.0)\{-0.356603\times10^{-6}\\
&+0.788212\times10^{-8}\theta+0.408195\times10^{-10}p\\
&-0.602281\times10^{-15}p^2\}+(S-35.0)^2\\
&\times\{+0.515032\times10^{-8}\}+p\{-0.121555\times10^{-7}\\
&+0.192867\times10^{-9}\theta-0.213127\times10^{-11}\theta^2\}\\
&+p^2\{+0.176621\times10^{-12}-0.175379\times10^{-14}\theta\}\\
&+p^3\{+0.121551\times10^{-17}\}.
\end{aligned}
$$

The units of β are $(psu)^{-1}$ and the rms error of this fit is 0.163 $\times$ 10^{-6} $(psu)^{-1}$. A test value is 0.72088 $\times$ 10^{-3} $(psu)^{-1}$ at S = 40.0 psu, θ = 10.0°C and p = 4000.0 db.

REFERENCES

Armi, L., and H. Stommel, 1983: Four views of a portion of the North Atlantic Subtropical Gyre. *J. Phys. Oceanogr.*, **13**, 828–857.

Bainbridge, A. E., 1976: *GEOSECS Atlantic Expedition, Vol. 2, Sections and Profiles.* National Science Foundation, Washington DC, 198 pp.

Broecker, W. S., and T-H. Peng, 1982: *Tracers in the Sea.* Columbia University Press, 690 pp.

Bryden, H. L., 1973: New polynomials for thermal expansion, adiabatic temperature gradient and potential temperature of seawater. *Deep-Sea Res.*, **20**, 401–408.

Ekman, V. W., 1934: Review of "Das Bodenwasser und die Gliederung der Atlantischen Tiefsee" by Georg Wust, published in Wiss. Ergebn. Dtsch. Atlant. Exped. 1925–1927, herausgeg. von A. Defant, Band VI, Teil I, Lief 1. Berlin andf Leipzig, 1932. *J. Cons. Perm. Int. Explor. Mer.* **9**(1), 102–104.

Fofonoff, N. P., 1985: Physical properties of seawater: A new salinity scale and equation of state for seawater. *J. Geophys. Res.*, **90**, 3332–3342.

——, and R. C. Millard, 1984: Algorithms for computation of fundamental properties of seawater, UNESCO, Paris. *Tech. Pap. Mar. Sci.*, **44**, 53 pp.

Gill, A. E., 1982: *Atmosphere-Ocean Dynamics.* Academic Press, 662 pp.

Ivers, W. D., 1975: The deep circulation in the northern North Atlantic, with especial reference to the Labrador Sea. Ph.D. thesis, Scripps Institute of Oceanography, University of California, San Diego.

Jenkins, W. J., 1987: ^3H and ^3He in the Beta Triangle: Observations of gyre ventilation and oxygen utilization rates. *J. Phys. Oceanogr.*, **17**, 763–783.

Levitus, S., 1982: *Climatological Atlas of the World Ocean.* National Oceanic and Atmospheric Administration, U.S. Department of Commerce, Prof. Paper 13.

Lynn, R. J., and J. L. Reid, 1968: Characteristics and circulation of deep and abyssal waters. *Deep-Sea Res.*, **15**, 577–598.

Mamayev, O. I., 1975: *Temperature-Salinity Analysis of World Ocean Waters.* English version, Elsevier, 374 pp.

McDougall, T. J., 1984: The relative roles of diapycnal and isopycnal mixing on subsurface water mass conversion. *J. Phys. Oceanogr.*, **14**, 1577–1589.

——, 1987: Thermobaricity, cabbeling and water mass conversion. *J. Geophys. Res.*, **92**, 5448–5464.

Montgomery, R. B., 1938: Circulation in the upper layers of the southern North Atlantic, deduced with the use of isentropic analysis. *Pap. Phys. Oceanogr. Meteor.*, **6**(2), 55 pp.

Pingree, R. D., 1972: Mixing in the deep stratified ocean. *Deep-Sea Res.*, **19**, 549–561.

Reid, J. L., 1981: On the mid-depth circulation of the World Ocean. In *Evolution of Physical Oceanography.* B. A. Warren, and C. Wunsch, Eds. 70–111.

——, and R. J. Lynn, 1971: On the influence of the Norwegian–Greenland and Weddell Seas upon the bottom waters of the Indian and Pacific Oceans. *Deep-Sea Res.*, **18**, 1063–1088.

Sgouros, T. A., and T. Keffer, 1983: The CAMS interactive Atlas package: A computerized program for the archiving and presentation of oceanographic data. Woods Hole Oceanographic Institution, Tech. Rep. WHOI-83-39.

Takahashi, T., W. S. Broecker and S. Lauger, 1985: Redfield ratio based on chemical data from isopycnal surfaces. *J. Geophys. Res.*, **90**, 6907–6924.

Wust, Georg, 1933: Das Bodenwasser und die Gliederung der Atlantischen Tiefsee. *Wiss. Ergebn. Dtsch. Atlant. Exped. "Meteor"*, **6**(I), (1): 1–107. (Teil I: Schichtung und Zirkulation des Atlantischen Ozeans.)